International Conference on Applied Energy 2019
Aug 12-15, 2019, Västerås, Sweden
Paper ID: 0275

TRANSIENT STABILITY ANALYSIS OF POWER SYSTEM WITH DFIG BASED ON TRANSIENT ENERGY FUNCTION METHOD

Huilan Jiang[1*], Jizhao Cai[1], Yuling Bai[1]
1 Key Laboratory of Smart Grid of Ministry of Education (Tianjin University), Nankai Distric, Tianjin, 300072, China

ABSTRACT

The impact of large-scale wind power integration on the stable operation of power system has attracted great attention. This paper presents a method to analyze the influence of doubly-fed induction generation (DFIG) on the power system transient stability by using transient energy function. The transient energy function of the system with DFIG is constructed based on the rotor equation of the system by introducing the equivalent parallel grounded admittance model of DFIG and the critical energy of the system is given. Furtherly, the effect of DFIG on the system transient stability margin is analyzed. In addition, combined the influence of DFIG on the change of system state variables with the energy accumulation process during the fault, the influence mechanism and quantitative analysis of the DFIG on the system critical clearing time and transient power angle variation of synchronous machines are realized. In the simulation analysis, two different LVRT schemes of DFIG are compared, and the simulation results verify the correctness of the proposed method.

Keywords: transient stability, doubly-fed induction generation (DFIG), transient energy function (TEF), stability margin, critical clearing time (CCT), LVRT

1. INTRODUCTION

In recent years, the installed capacity of wind power has been continuously improved, and large-scale wind power integration has caused the structural change of the power grid and greatly affected the transient stability of the system [1-2]. The DFIG is widely used in wind farm due to its excellent asynchronous operation ability and smaller converter capacity. At present, many scholars have studied the impact of doubly-fed wind farm integration on transient stability of power system [3-6].

In [3], the transient stability of the system with constant speed wind turbine and DFIG are simulated respectively. The results show that the system with DFIG is more robust. The influence of DFIG connected to the system at different locations is analyzed in [4], which concludes that the impact of DFIG on transient stability of system varies with different integration locations. It can be seen that the influence degree of DFIG on the transient stability of the system should be determined according to the specific situation. Therefore, it is of great practical significance to carry out theoretical analysis methods. In [5], the mechanical and electromagnetic power of DFIG are converted into the change of the equivalent mechanical power of the system, and the variation of the power angle of the system is analyzed by the equal area criterion. However, DFIG does not have the electromechanical transient process, which means its mechanical power does not participate in the change of the system motion state. In [6], the TEF of system with DFIG is constructed, and the influence of DFIG on the system energy margin is analyzed when the voltage drop depth is different. The method considers that the change of the energy margin of the whole system is to increase the energy limit that the DFIG can withstand in the transient process. However, the DFIG changes the original state and topology of the system, the original energy margin of the system will also change accordingly. It is necessary to analyze the influence of DFIG on the system's stability margin or the CCT reflecting the stability of the system, which is more significant for engineering practice.

Aiming at the above insufficiency, this paper proposes a method to analyze the influence of DFIG integration on the transient power angle stability of system by using TEF, and the influence mechanism of DFIG on transient stability is analyzed, so that the CCT

Selection and peer-review under responsibility of the scientific committee of the 11th Int. Conf. on Applied Energy (ICAE2019).

and transient power angle can be quantified. By introducing the equivalent parallel grounded admittance model of DFIG, the general expression of TEF of system with DFIG is constructed. The effect of DFIG on the stability margin of the system is analyzed quantitatively by using critical energy. Besides, the influence of DFIG on the electromagnetic power of synchronous machine during the fault is used to analyze the change of state variables and the energy accumulation process of the system. And the CCT is calculated by the accumulation time from transient energy to critical energy of the system, which can represent the overall stability of the system. The method proposed in this paper takes into account the influence of DFIG on the system stability margin and the system power angle during LVRT and provides an effective way for the actual demand analysis of the influence of DFIG integrated on the transient power angle stability of the system.

2. TEF OF THE SYSTEM WITH DFIG

2.1 The influence mode of DFIG on system transient power angle stability

The DFIG's electrical and mechanical parts are decoupled, which makes DFIG does not have the electromechanical characteristics as synchronous machines. The change of DFIG in electromagnetic power is not the subject of the system transient stability. The DFIG can be regarded as introducing a non-autonomous factor into the system, which is the active and reactive power of the DFIG output. Therefore, the external power characteristics of the DFIG can be represented by equivalent parallel ground conductance and susceptance, as shown in Figure 1.

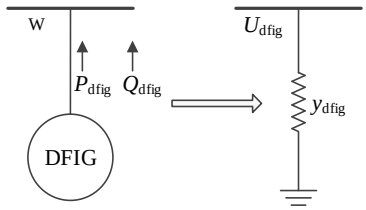

Figure 1 Equivalent grounded admittance reflecting DFIG power characteristics

According to the circuit principle, the expression of the grounded admittance is as follows:

$$y_{\mathrm{dfig}} = -g_{\mathrm{dfig}} + \mathrm{j}b_{\mathrm{dfig}} = -\frac{P_{\mathrm{dfig}}}{U_{\mathrm{dfig}}^2} + \mathrm{j}\frac{Q_{\mathrm{dfig}}}{U_{\mathrm{dfig}}^2} \tag{1}$$

Where P_{dfig} and Q_{dfig} are the active power and reactive power output from the DFIG to the system, and U_{dfig} is the terminal voltage value of the DFIG.

2.2 Construction of TEF

The system with DFIG is shown in Figure 2.

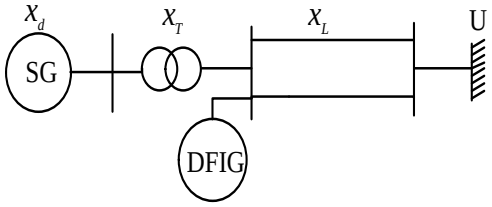

Figure 2 Diagram of system with DFIG

Where x_d stands for the transient reactance of the synchronous machine, x_T stands for the reactance of the transformer, x_L stands for the reactance of the single-circuit transmission line.

Assuming that the damping is not included, the infinite bus is used as the slack bus in the system. The equation of motion of the system represented in Figure 2 can be represented by the following second-order differential equation:

$$M\frac{\mathrm{d}^2\delta}{\mathrm{d}t^2} = P_{\mathrm{m}} - P_{\mathrm{e.i}} \ , \ i = 1,2,3 \tag{2}$$

Where M is the inertia time constant of the synchronous generator; δ is the rotor angle of the synchronous machine; P_m is the mechanical power of the synchronous machine; $P_{e.i}$ is the electromagnetic power output for the synchronous machine; i is the time interval number, when $i = 1$, it stands for the steady-state phase before the fault; when $i = 2$, it stands for that it is in the fault process; when $i = 3$, it stands for the phase after the fault clears.

The simplified circuit of the system after the fault is shown in Figure 3.

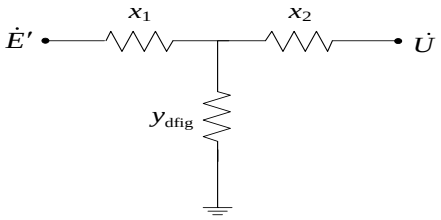

Figure 3 Equivalent circuit diagram of the system after fault

Where $x_1 = x_d + x_T$ and $x_2 = x_L$ are the line parameter; $\dot{E}'$ is the transient potential; $\dot{U}$ is the voltage phasor for the infinite bus; y_{dfig} is the equivalent ground admittance of DFIG.

According to the circuit diagram, the general formula of electromagnetic power of synchronous machine after fault can be expressed as [7]:

$$P_{e3}=\frac{E'^2}{|Z_{11}|}\sin\alpha_{11}+\frac{E'U}{|Z_{12}|}\sin(\delta-\alpha_{12}) \tag{3}$$

Where δ is the angle difference between $\dot{E}'$ and $\dot{U}$, that is, the equivalent power angle of the system; Z_{11} and Z_{12} are the transfer impedance of the system respectively; α_{11} is the angle between the self-impedance and the self-reactance in the self-impedance triangle; α_{12} is the angle between the mutual impedance and the mutual reactance. Among them, each parameter is represented as:

$$\begin{cases} Z_{11}=\mathrm{j}x_1+\left(\dfrac{1}{y_{\mathrm{dfig}}}\right)//\mathrm{j}x_2=|Z_{11}|\angle\varphi_{11} \\ \alpha_{11}=\dfrac{\pi}{2}-\varphi_{11} \\ Z_{12}=\mathrm{j}x_1+\mathrm{j}x_2-x_1x_2y_{\mathrm{dfig}}=|Z_{12}|\angle\varphi_{12} \\ \alpha_{12}=\dfrac{\pi}{2}-\varphi_{12} \end{cases} \tag{4}$$

The power angles δ_1 and δ_2 corresponding to the stable equilibrium point and the unstable equilibrium point of the system equation (2) can be solved by the equation $P_{\mathrm{m}}-P_{e3}=0$.

The stable equilibrium point of the system after the fault is converted to the origin, that is, $y_1=y=\delta-\delta_1$, $y_2=\dot{y}=\dot{\delta}=\omega-\omega_1$. Then the system equation can be expressed as:

$$\begin{cases} \dot{y}_1=y_2=g_1(y_1,y_2) \\ \dot{y}_2=-\dfrac{f(y_1)}{M}=g_2(y_1,y_2) \end{cases} \tag{5}$$

Formula (5) satisfies the necessary and sufficient conditions for solving the theorem of the first integral, for the first integral of Formula (5), and substituting $y_1=\delta-\delta_1$ and $y_2=\omega-\omega_1$ into it ,the following expression can be obtained:

$$\begin{aligned} V(\delta,\omega)=&\frac{1}{2}M(\omega-\omega_1)^2-\left(P_{\mathrm{m}}-\frac{E'^2}{|Z_{11}|}\sin\alpha_{11}\right)(\delta-\delta_1) \\ &-\frac{E'U}{|Z_{12}|}\left[\cos(\delta-\alpha_{12})-\cos(\delta_1-\alpha_{12})\right] \end{aligned} \tag{6}$$

Formula (6) is the TEF of the system with DFIG expressed by state variables (δ,ω). Among them, the first item represents the transient kinetic energy of the system, and the other items represent the transient potential energy of the system.

3. TRANSIENT STABILITY ANALYSIS BASED ON TEF

3.1 Critical energy of system with DFIG

In order to solve system's CCT, which is an index to quantify the transient power angle stability, it is necessary to analyze the critical energy of the system. When the rotor moves to the operating point δ_2, the system reaches an unstable equilibrium point, which means that the system reaches the maximum potential energy that can be withstood. Therefore, the critical energy of the system is the transient potential energy under the unstable equilibrium operating point:

$$\begin{aligned} V_{\mathrm{cr}}=V(\delta_2,\omega_2)=&-\left(P_{\mathrm{m}}-\frac{E'^2}{|Z_{11}|}\sin\alpha_{11}\right)(\delta_2-\delta_1) \\ &-\frac{E'U}{|Z_{12}|}\left[\cos(\delta_2-\alpha_{12})-\cos(\delta_1-\alpha_{12})\right] \end{aligned} \tag{7}$$

Through the calculation of equation (4), the change of the DFIG integrated to the system network structure can be transformed into the change to the network parameters of the system. Therefore, it can be seen from the expression (7) of the critical energy that the DFIG changes the critical energy of the system, thereby affecting the transient stability margin of the system.

3.2 Influence mechanism of DFIG integrated on system transient energy accumulation process

Different LVRT schemes make the power output of the DFIG change, which causes the different influences on the electromagnetic power of the synchronous machine, and further causes difference in the way the system state variables change. From the perspective of the energy function, the active and reactive power transmitted by the DFIG to the grid during the fault change. The electrical connection between the grid connection point of the DFIG and the system affects the electromagnetic power of the synchronous machine, further affecting the way of the system state variables change, thereby changing the accumulation process of the transient energy of the system.

Assuming that the voltage at the DFIG exit drops to u_{dfig} and there is a smaller grounding resistance *r* at the fault location. z_{dfig} and y_{dfig} are reciprocals each other. The expressions of the system transfer impedances Z_{11} and Z_{12} during the fault are as follows:

$$\begin{cases} Z_{11}=\mathrm{j}x_1+\left(z_{\mathrm{dfig}}//r\right)//\mathrm{j}x_2=\mathrm{j}x_1+\dfrac{u^2rx_2}{x_2\left(u^2-rp+\mathrm{j}rq\right)-\mathrm{j}u^2r} \\ Z_{12}=\mathrm{j}x_1+\mathrm{j}x_2+\dfrac{\mathrm{j}x_1\cdot\mathrm{j}x_2}{z_{\mathrm{dfig}}//r}=\mathrm{j}(x_1+x_2)-\dfrac{x_1x_2\left(u^2-rp+\mathrm{j}rq\right)}{u^2r} \end{cases} \tag{8}$$

In the process of fault, the expression of the electromagnetic power of the system is as follows：

$$P_{e2}=\frac{E'^2}{|Z_{11}|}\sin\alpha_{11}+\frac{E'U}{|Z_{12}|}\sin(\delta-\alpha_{12}) \quad (9)$$

Combining equations (8) and (9), it can be seen that the value of the electromagnetic power of the synchronous machine during the fault decreases as the DFIG output active power p increases, but increases as the DFIG output reactive power q increases.

Further, it is assumed that the active reactive power outputted by the DFIG during the fault is a fixed value. The relationship between the electromagnetic power of the synchronous machine and the system state variable is analyzed. In the shorter time period in which the fault persists, taking the average value of the electromagnetic power P_{e2} of the synchronous machine for calculation, and the rotor motion equation (2) of the system during the fault is integrated, and the integral interval is taken as (0, *t*), and the rotor angular velocity of the synchronous machine is as follows.

$$\omega(t)=\dot{\delta}(t)=\dot{\delta}(0)+\frac{P_m-P_{e2}}{M}t \quad (10)$$

The time variable t on both sides of the equation (10) is integrated, and the integral interval is still taken as (0, t). The rotor angle of the synchronous machine is as follows:

$$\delta(t)=\delta(0)+\frac{P_m-P_{e2}}{2M}t^2 \quad (11)$$

Therefore, it can be seen from equations (10) and (11) that, in the case where the fault duration *t* is the same, the larger the electromagnetic power output by the synchronous machine, the smaller the values of the rotor angle and the rotor angular velocity of the synchronous machine, which inevitably makes the system's transient kinetic energy and transient potential energy smaller, then makes the system more stable. In other words, the more the electromagnetic power output by the synchronous machine, the longer for the system to accumulate the transient energy to reach the critical energy, reflecting that the system is more stable.

3.3 Quantitative analysis of the CCT

By substituting the equations (10) and (11) into the expression (6) of the TEF, a unary function of the energy function with respect to the time variable can be obtained:

$$V(t)=\frac{1}{2}M(\omega_0+\frac{P_m-P_{e2}}{M}t-\omega_1)^2-\left(P_m-\frac{E'^2}{|Z_{11}|}\sin\alpha_{11}\right)\left(\delta_0+\frac{P_m-P_{e2}}{2M}t^2-\delta_1\right)+\frac{E'U}{|Z_{12}|}\left[\cos\left(\delta_0+\frac{P_m-P_{e2}}{2M}t^2-\alpha_{12}\right)-\cos(\delta_1-\alpha_{12})\right] \quad (12)$$

When the value of the above function reaches the critical energy value obtained by equation (7), that is $V(t)=V_{cr}$, the time corresponding to the system is the CCT of the system. The quantitative analysis of the influence degree of wind power integration on the transient power angle stability of the system is realized.

4. EXAMPLE ANALYSIS

The simulation model is built in Simulink. The fault start time is set to 0.2s, the grounding resistance is set to $10\ \Omega$, and the DFIG grid point voltage drop depth is 80%. The system reference capacity is set to S_B=100MVA, and the reference voltage U_B is set to the rated voltage of each voltage level.

4.1 The effect of DFIG integrated on critical energy

Firstly, combining the network parameters of the system with equations (3) and (7), it is calculated that after the fault resection of the system without DFIG, the power angle at the stable equilibrium point and the critical energy of the system are $\delta^s_{SMIB}=0.4964$ and $V_{cr\_SMIB}=0.5348$ respectively. Use the graphical method to find the system's CCT=0.098s as shown in Figure 4(a).

The simulation result is shown in Figure 4(b). It is concluded that the CCT of a single-machine infinite system is between 0.11s and 0.12s, which is similar to the calculated result.

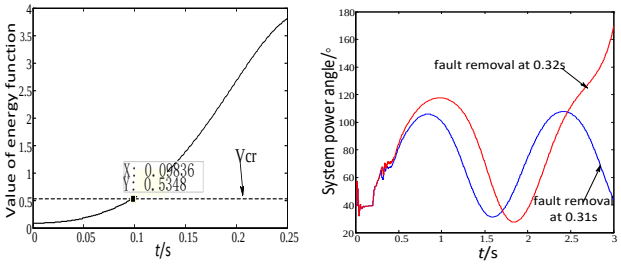

a calculation result b simulation result

Figure 4 CCT calculation and simulation results without DFIG system

It is calculated that the power angle of the system with DFIG at the stable equilibrium point after fault removal and the critical energy of the system are $\delta^s=0.6758$ and $V_{cr}=1.7484$ respectively. It can be seen that DFIG enhances the maximum transient energy limit and the limit of the system's stability tolerance.

4.2 Influence of different LVRT schemes on energy accumulation process

This paper uses DFIG's stator series reactance integrated LVRT strategy [8] (scheme A) and the traditional crowbar LVRT strategy (scheme B) to verify. The difference between the two LVRT schemes is that the stator series reactance mode can provide the

reactive power that meets the LVRT requirements, while the rotor-side converter of the DFIG is locked in the crowbar mode, so the reactive power is absorbed from the system during the LVRT.

Taking the fault time from 0.2 to 0.44 s, according to the active and reactive power comparison diagrams of the two LVRT schemes (Figure 5), the average values of the active and reactive outputs of the DFIG under the two LVRT schemes are calculated as $P_{\mathrm{A}}=0.1494,\ Q_{\mathrm{A}}=0.1227$ and $P_{\mathrm{B}}=0.0958,\ Q_{\mathrm{B}}=-0.0684$ respectively.

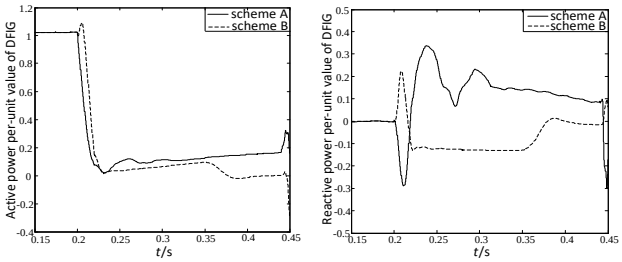

Figure 5 DFIG active and reactive power comparison under different LVRT schemes

Combined with (8) and (9), the average values of the electromagnetic power of the synchronous machine during the fault are $P_{\mathrm{e2\_A}}$=0.3615 and $P_{\mathrm{e2\_B}}$=0.1867 respectively. The CCTs of the system using two different schemes are $\mathrm{CCT_A}$=0.3044s and $\mathrm{CCT_B}$=0.222s respectively by using the graphical method. The theoretical calculation results show that the electromagnetic power of the synchronous machine of scheme A is larger than that of the scheme B during the fault, and the CCT of the system is larger, indicating that the scheme A is more conducive to the transient stability.

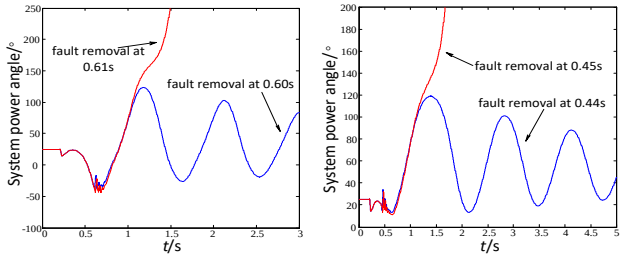

a scheme A b scheme B

Figure 6 Power angle simulation results of the system under different schemes

Figure 6 shows the simulation results of the system power angle. It can be seen that when using scheme A, the CCT of the system is between 0.40 and 0.41s, and when scheme B is used, the CCT of the system is between 0.24 and 0.25 s. The simulation results are similar to the calculation results, indicating that the applicability of the energy function method is great.

5. CONCLUSIONS

(1) By translating the influence of DFIG integrated on the network topology into on the network parameters, the influence of DFIG on the system stability margin can be quantified;

(2) DFIG not only changes the stability margin of the system, but also changes the state variables of the system by affecting the electromagnetic power of the synchronous machine during the fault, thereby affecting the speed of transient energy accumulation.

ACKNOWLEDGEMENT

This work was supported by the National Natural Science Foundation of China under Grant No.51477115.

REFERENCE

[1] Siwei Liu, Gengyin Li, Ming Zhou. Impact analysis of doubly-fed induction generator on the transient angle stability of the region with wind power integrated. Power System Protection and Control 2016; 44(6): 56-61.

[2] Mingli Zhang, Jianyuan Xu, Jiayu Li. Research on transient stability of sending power grid containing high proportion of wind power. Power System Technology 2013; 37(3): 740-745.

[3] Nunes M, Lopes J, Zurn H, et al. Influence of the variable-speed wind generators in transient stability margin of the conventional generators integrated in electrical grids. IEEE Transactions on Energy Conversion 2004; 19(4): 692-701.

[4] Shi L, Dai S, Ni Y, et al. Transient stability of power systems with high penetration of DFIG based wind farms. IEEE Power & Energy Society General Meeting, Calgary, Canada; 2009.

[5] Li Lin, Yihan Yang. Analysis of transient stability of power system including large scale wind power based on the extended equal area rule. Power System Protection and Control 2012; 40(12): 105-110.

[6] Chowdhury M A, Shen W, Nasser H, et al. Transient stability of power system integrated with doubly fed induction generator wind farms. IET Renewable Power Generation 2015; 9(2): 184-194.

[7] Qiang Yu. Study on the transient angle stability of power system with doubly-fed induction generator integrated. Beijing: China Electric Power Research Institute; 2013.

[8] Huilan Jiang, Tianpeng Li, Yuzhang Wu. Integrated Strategy for Low Voltage Ride Through of Doubly-fed Induction Generator. High Voltage Engineering 2017; 6(43): 2062-2068.